Performance Improvement of a One-DOF Actively Positioned Bearingless Motor

Junichi Asama*
Shizuoka University
Hamamatsu, Japan

Takaaki Oiwa
Shizuoka University
Hamamatsu, Japan

Akira Chiba
Tokyo Institute of Technology
Tokyo, Japan

Abstract

Conventional bearingless motors and magnetic bearings with one- to five-degrees-of-freedom (DOF) active positioning require a number of inverter modules, windings, position sensors, and electromagnets. To reduce the size and power consumption of this type of motor, the authors previously proposed a one-DOF actively positioned bearingless motor, referred to as a single-drive bearingless motor that has only one three-phase winding set and one three-phase inverter. Although the successful non-contact operation of this motor was demonstrated previously, a rotor of the test machine ran up to only 800 r/min because of serious resonance. The aim of this study was to improve the rotation performance of the single-drive bearingless motor. The cause of the rotor vibration was a discontinuous distribution of the magnetic flux density in the air-gap. One possible solution has been proposed in this paper. The test machine with an improved rotor was successfully driven up to 2000 r/min.

1 Introduction

An active magnetic bearing suspends a rotating shaft regulating suspension force without any mechanical contact [1]. To rotate the shaft, an additional motor element is installed in the magnetic bearing system. On the other hand, a bearingless motor generates both suspension force and torque in a single unit [2]. The advantages of these bearingless rotating machines are high-speed and lubricant-free operation, no wear particles, no material wear, and less heat generation. To realize non-contact magnetic suspension of the rotor, it must be magnetically stabilized in five- degrees-of-freedom (DOF), which includes three- translational (x, y, z) and two- tilting (θ_x, θ_y) motions but not a rotating direction (θ_z).

A general four-DOF actively positioned bearingless motor has two bearingless motor units constructed in tandem, where radial (x, y) and tilting (θ_x, θ_y) motions are actively controlled [3-5]. An axial motion (z) of the rotor is passively stabilized with magnetic couplings between the rotor and the stator. Three-phase motor windings are commonly wound around stators of two bearingless motor units, although additional suspension windings are wound around respective stators. Thus, one three-phase inverter is required for torque generation, and two additional three-phase inverters are required for four-DOF active suspension. In a five-DOF actively positioned bearingless drive system, a thrust magnetic bearing is additionally installed into the four-DOF-positioned bearingless motor [6, 7]. An additional single-phase inverter is required for thrust motion control. In a two-DOF-positioned bearingless motor, the radial motion (x, y) of the rotor is actively controlled [8-12]. The remaining DOFs (z, θ_x, θ_y), except for the rotational motion (θ_z), are passively stabilized. To successfully realize non-contact operation, two displacement sensors, two sets of three-phase windings, and two three-phase inverters are required. Alternatively, two displacement sensors, one set of four- or five-phase windings, and one four- or five-phase inverter are required [13, 14].

An increase in the number of actively controlled DOFs causes increases in size, power consumption, and cost, and it complicates the system control. To solve these problems, one-DOF actively controlled magnetic bearings have been proposed [15-17]. In these test machines, the magnetic suspension and rotating parts are separated. Both single-phase and three-phase inverters are required for axial force and torque regulation, respectively. Ueno *et al*. have proposed an axial-gap bearingless motor with one-DOF active regulation, where an axial force is only regulated for non-contact magnetic suspension [18-20]. However, two sets of inverters are necessary for complete magnetic suspension of the rotor.

*Contact Author Information: tjasama@ipc.shizuoka.ac.jp, 3-5-1 Johoku, Naka-ku, Hamamatsu 432-8561, Japan, Tel: +81-53-478-1033, Fax: +81-53-478-1041

We previously proposed a novel concept of a one-DOF actively positioned bearingless motor, referred to as a single-drive bearingless motor [21]. It has only one three-phase winding set and one three-phase inverter for both non-contact magnetic suspension and rotation. Although the successful non-contact operation has previously been demonstrated, a rotor of the prototype machine runs only up to 800 r/min because of undesirable resonance of the rotor. The aim of this study was to improve the rotation performance of the single-drive bearingless motor. We determined that the vibration was caused by a discontinuous distribution of the magnetic flux density in the air-gap. One possible solution has been proposed, and its effectiveness is verified in the prototype motor with an improved rotor.

2 Single-Drive Bearingless Motor

Figure 1 shows the structure of a single-drive bearingless motor. Axial motion of the rotor (z) is actively positioned by regulating the suspension force. Other DOFs (x, y, θ_x, θ_y) are passively stabilized. Two axial-gap surface-mounted permanent magnet motors are combined. Rotor cores are connected with a shaft. A ring-shaped permanent magnet is attached on the rotor iron surface at both ends. One stator has a general three-phase winding for both rotation and magnetic suspension. No additional winding is required for active magnetic suspension control. In Figure 1, the stator has six teeth with concentrated winding configuration and provides a two-pole rotating magnetic field to drive and suspend the two-pole rotor. A displacement sensor is installed at the center of the stator core to detect the rotor axial motion.

Figure 2 shows a principle of suspension force generation in the axial direction. The permanent magnet generates bias magnetic flux, resulting in closed magnetic couplings between the rotor and the stator. When the rotor is positioned at the center, where the axial gaps of both rotor ends are equal, positive and negative attractive forces in the axial direction are equal. As shown in Figure 2(a), field strengthening causes an increase in the attractive force in the positive axial direction, resulting in positive suspension force. In a similar manner, field weakening generates a negative suspension force, as shown in Figure 2(b).

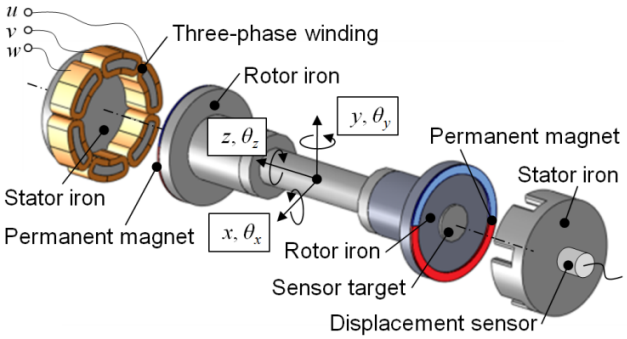

Figure 1: Structure of a single-drive bearingless motor

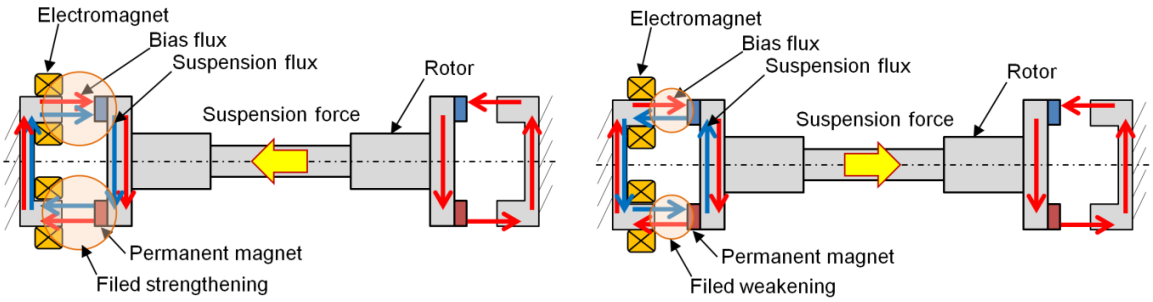

(a) Field strengthening (b) Field weakening

Figure 2: Principle of suspension force generation in the axial direction

Figure 3 shows a principle of passive stabilization of the rotor in the radial (x, y) and tilting (θ_x, θ_y) directions. The magnetic couplings between the rotor and the stator contribute to the passive stabilization. When the rotor moves in the radial direction, a resulting restoring force pulls the rotor back to the center position, as shown in Figure 3(a). In a similar manner, the rotor tilting movement causes a restoring torque, with the rotor eventually converging in the nominal position, as shown in Figure 3(b).

Figure 4 shows a control block of the single-drive bearingless motor. Positive and negative d-axis currents control the field strengthening and weakening in the air-gap, respectively. A proportional-integral-derivative (PID) feedback loop stabilizes the axial rotor motion by regulating the d-axis suspension current, i_d. Rotational torque is controlled by regulating the q-axis current, i_q. To regulate the d- and q-axis currents, the PI feedback loops are adopted. The d- and q-axis voltage commands are transformed into the a- and b-axis voltage commands v_a* and v_b*. These are then transformed into the three-phase voltage references v_u*, v_v*, and v_w*. The three-phase voltage source inverter is controlled by the three-phase voltage commands and supplies the suspension-winding currents i_u, i_v, and i_w. Both rotational torque and magnetic suspension force are generated for rotational speed regulation and active Z-axis positioning by regulating the q- and d-axis currents, respectively. Thus, the single-drive bearingless motor can be driven by only one three-phase inverter and one three-phase winding set.

Figure 5 shows a test machine of the single-drive bearingless motor. The rotor and stator cores are made of bulk soft iron. Four segmented permanent magnets with an arc angle of 90° are used to construct a circular shape. The permanent magnets are made of NdFeB with a residual flux density of 1.2 T. The axial thickness and radial width of the permanent magnet are 0.5 mm and 2 mm, respectively. A magnetic air-gap between surfaces of the permanent magnet and stator teeth is 0.6 mm. A short-pitch concentrated winding is used with a copper wire diameter of 0.16 mm. An axial rotor motion is measured with an eddy-current-type displacement sensor (PU-03A, AEC Corp., Japan). The rotating angular position is detected by two Hall elements. A voltage source three-phase pulse-width-modulation (PWM) inverter with a DC voltage of 36 V is controlled by a digital micro-processor (SH7047, Renesas Technology Corp., Japan). The sampling rates for the suspension control and current control are 300 μs and 100 μs, respectively.

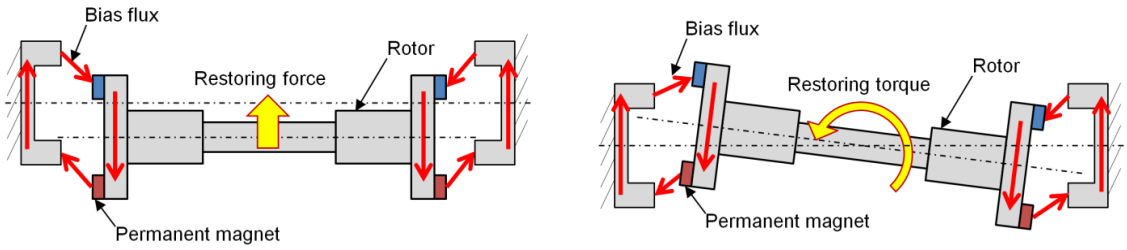

(a) Radial direction (b) Tilting direction

Figure 3: Principle of four-DOF passive suspension

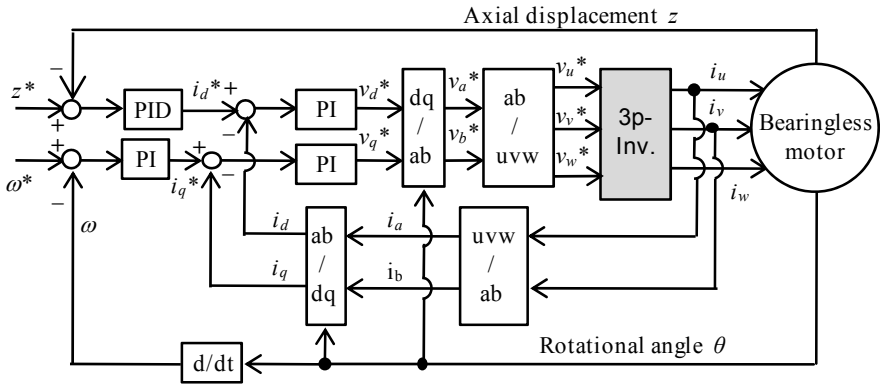

Figure 4: Control block of single-drive bearingless motor

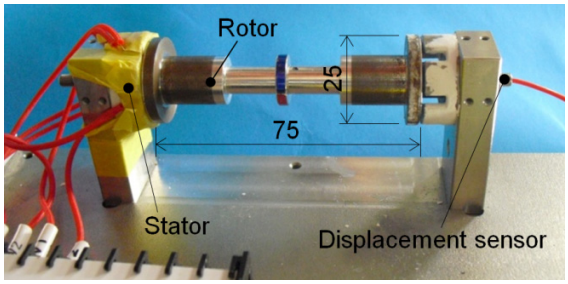

Figure 5: Fabricated single-drive bearingless motor

3 Performance Improvement

Although the successful non-contact operation of our single-drive bearingless motor has been demonstrated, a rotor of the prototype machine runs only up to approximately 800 r/min (13.3 Hz). The rotor vibration increases with an increase in the rotational speed, eventually resulting in touch-down, although the measured radial and conical resonant frequencies are 30.2 Hz (1810 r/min) and 29.8 Hz (1790 r/min), respectively. Figure 6 shows measured rotor vibration in the radial and tilting directions with a conventional rotor at 790 r/min. The rotor motion in these directions is passively stabilized by the magnetic couplings between the rotor and the stator. The rotor vibration is measured using two laser triangulation displacement sensors (HL-C2, Panasonic Corp., Japan). In both waveforms, fundamental (13.1 Hz) and second harmonic (26.2 Hz) components are observed by fast-Fourier-transform (FFT) analysis. The frequency of the second harmonic gradually reaches both the radial and conical resonant frequencies. In particular, conical resonance causes significant rotor vibration that limits the maximum rotational speed. Therefore, we carefully investigated the cause of the second harmonic generation.

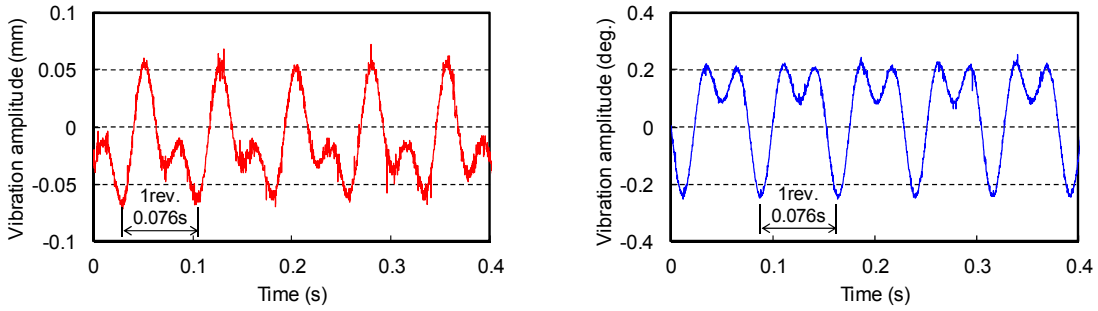

(a) Radial direction (b) Tilting direction

Figure 6: Rotor vibration in the tilting direction with a conventional rotor at 790 r/min

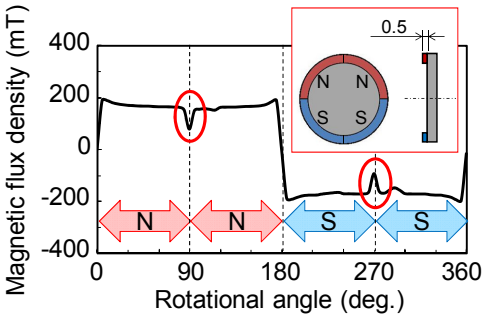

Figure 7: Measured flux distribution on the surface of the permanent magnet with a conventional rotor

Figure 7 shows the measured distribution of magnetic flux density on the surface of the segmented permanent magnets. The conventional rotor structure is also indicated in Figure 7. The flux density instantaneously changes around the middle point in each pole region because of the boundary of the permanent magnet pieces. This discontinuous flux distribution may cause the second harmonic vibration.

To improve the maximum rotational speed and reduce the second harmonic component, we improved the rotor structure. Two segmented permanent magnets with an arc angle of 180° are alternatively used. Figure 8 shows the measured distribution of magnetic flux density on the surface of the segmented permanent magnets when the improved rotor is used. The axial thickness of the permanent magnet is increased to 1 mm for an increase in mechanical strength. The axial magnetic air-gap between the surfaces of the permanent magnet and the teeth is also changed to 1 mm. Instantaneous changes around the middle point in each pole region disappear when these changes are made, as shown in Figure 8. Figure 9 shows both a conventional rotor and an improved rotor. The improved rotor weighs 40 % less. The measured resonant frequencies of the improved rotor in the radial and tilting directions are 38.1 Hz (2290 r/min) and 36.8 Hz (2200 r/min), respectively.

Figure 10 shows vibration amplitudes of the improved rotor in the radial and tilting directions in comparison to those of the conventional rotor. The improved rotor is driven up to approximately 2000 r/min. The maximum rotational speed is significantly improved, although the improved rotor touches down at more than 2000 r/min. Figure 11 shows the measured rotor vibration in the radial and tilting directions with an improved rotor at 2050 r/min (34.2 Hz). In these waveforms, a second harmonic component is not observed. Two segmented permanent magnets successfully contribute to the reduction of the second harmonic component of the conical vibration. At this stage of the research project, no special effort is being devoted to damping improvement, further vibration suppression, or the avoidance of conical resonance. These issues will be addressed in the future.

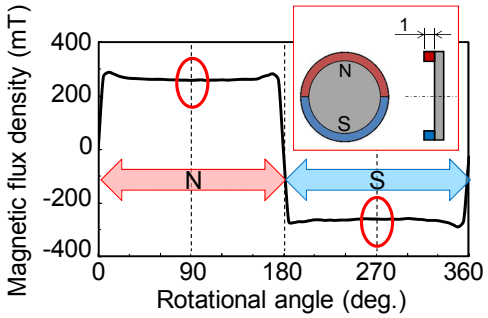

Figure 8: Measured flux distribution on the surface of the permanent magnet with an improved rotor

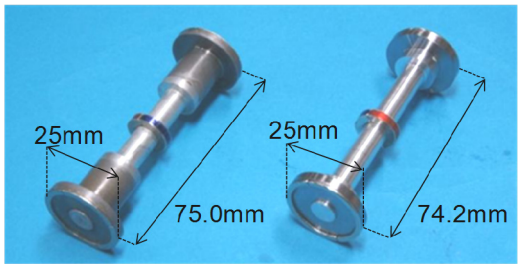

Figure 9: Conventional (left) and improved (right) rotors

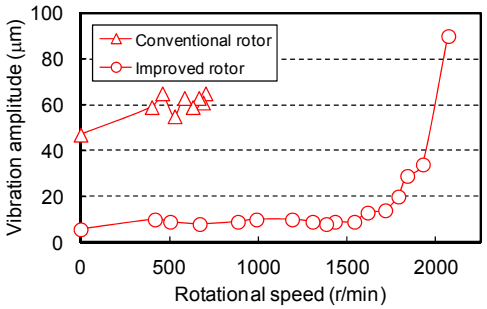

(a) Radial direction

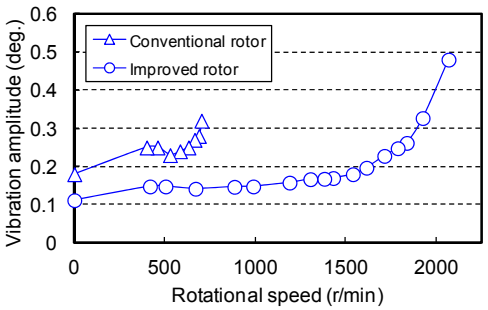

(b) Tilting direction

Figure 10: Vibration amplitudes of the rotor in the radial and tilting directions

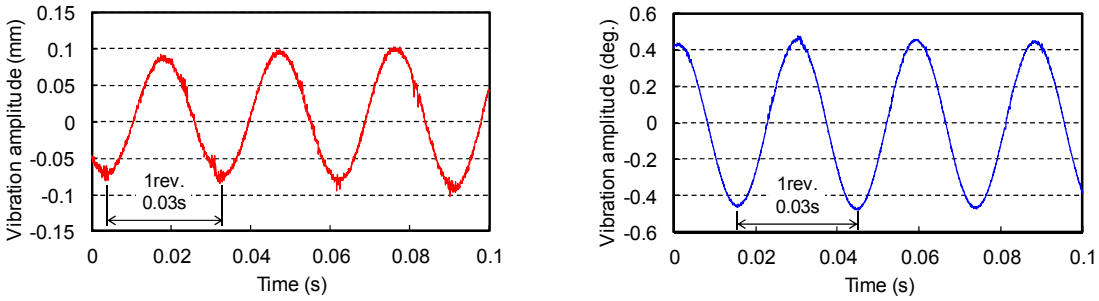

(a) Radial direction (b) Tilting direction

Figure 11: Rotor vibration in the tilting direction with an improved rotor at 2050 r/min

4 Conclusions

In this paper, improved performance of the single-drive bearingless motor has been shown. A conventional rotor with four segmented permanent magnets is driven at up to only 800 r/min because of the conical resonance resulting from the second harmonic vibration. Alternatively, two segmented permanent magnets are used to reduce the second harmonic vibration. The improved rotor is driven at up to 2000 r/min. Damping improvement, further vibration suppression, and the avoidance of conical resonance will be addressed in future works.

Acknowledgement

The authors would like to acknowledge the contribution to this research project of Mr. Yuki Hamasaki, a former graduate student in the Department of Mechanical Engineering, Graduate School of Engineering, Shizuoka University, Japan. This work was partly supported by Grants-in-Aid for Scientific Research of Japan Society for the Promotion of Science (23686041) and the NSK Foundation for the Advancement of Mechatronics.

References

[1] G. Schweitzer, E. H. Maslen, *et., al.*. Magnetic Bearings, Springer, 2009, ISBN: 978-3642007964.

[2] A. Chiba, T. Fukao, *et., al.*. Magnetic Bearings and Bearingless Drives, Newnes, 2005, ISBN: 978-0750657273

[3] Y. Asano, A. Mizuguchi, M. Amada, J. Asama, A. Chiba, M. Ooshima, M. Takemoto, T. Fukao, O. Ichikawa, and D. G. Dorrell. Development of a 4-axis Actively Controlled Consequent-Pole Type Bearingless Motor, IEEE Transactions on Industry Applications, Vol. 45, Issue 4, pp. 1378-1386, July/August 2009.

[4] J. Asama, R. Natsume, H. Fukuhara, T. Oiwa, and A. Chiba. Optimal Suspension Winding Configuration in a Homo-polar Bearingless Motor, IEEE Transactions on Magnetics (in press).

[5] A. Chiba and J. Asama. Influence of Rotor Skew in Induction type Bearingless Motor, IEEE Transactions on Magnetics (in press).

[6] M. Takemoto, S. Iwasaki, *et. al.*. Experimental Evaluation of Magnetic Suspension Characteristics in a 5-axis Active Control Type Bearingless Motor without a Thrust Disk for Wide-gap Condition, in Proceedings of the 2009 IEEE Energy Conversion Congress and Exposition, pp. 2362-2367, San Jose, USA, Sep. 2009.

[7] J. Asama, M. Amada, *et., al.*. Evaluation of a Bearingless PM Motor with Wide Magnetic Gaps, IEEE Transactions on Energy Conversion, Vol. 25, No. 4, pp. 957-964, December 2010.

[8] R. Schöb and N. Barletta. Principle and Application of a Bearingless Slice Motor, JSME (The Japan Society of Mechanical Engineers) International Journal, Series C, Vol. 40, No. 4, pp. 593-598, 1997.

[9] T. Reichert, T. Nussbaumer, and J. W. Kolar. Bearingless 300 W PMSM for Bioreactor Mixing, IEEE Trans. Industry Electronics, Vol. 59, Issue 3, pp. 1376 - 1388, 2012.

[10] J. Asama, R. Kawata, T. Tamura, T. Oiwa, and A. Chiba. Reduction of Force Interference and Performance Improvement of a Consequent-Pole Bearingless Motor, Precision Engineering, Vol. 36, Issue 1, pp. 10-18, January 2012.
[11] J. Asama, T. Asami, T. Imakawa, A. Chiba, A. Nakajima, and M. A. Rahman. Effects of Permanent-Magnet Passive-Magnetic-Bearing on a 2-axis Actively Regulated Low-Speed Bearingless Motor, IEEE Transactions on Energy Conversion, Vol. 26, No. 1, pp. 46-54, March 2011.
[12] H. Sugimoto, K. Kamiya, R. Nakamura, J. Asama, A. Chiba, T. Fukao, and D. G. Dorrell. Design and Basic Characteristics of Multi-Consequent-pole Bearingless Motor with bi-tooth Main Poles, IEEE Transactions on Magnetics, Vol. 45, Issue 6, pp. 2795-2798, June 2009.
[13] M. T. Bartholet, T. Nussbaumer, S. Silber, and J. W. Kolar. Comparative Evaluation of Polyphase Bearingless Slice Motors for Fluid-Handling Applications, IEEE Transactions on Industry Applications, Vol. 45, No. 5, Sep/Oct 2009.
[14] W. Gruber, W. Amrhein, and M. Haslmayr. Bearingless Segment Motor With Five Stator Elements – Design and Optimization, IEEE Transactions on Industry Applications, Vol. 45, No. 4, pp. 1301-1308, Jul/Aug 2009.
[15] I. D. Silva and O. Horikawa. An Attraction-Type Magnetic Bearing with Control in a Single Direction, IEEE Transactions on Industry Applications, Vol. 36, No. 4, pp. 1138-1142, Jul/Aug 2000.
[16] J. Kuroki, T. Shinshi, L. Li, and A. Shimokohbe. Miniaturization of a one-axis-controlled magnetic bearing, Precision Engineering, Vol. 29, Issue 2, pp. 208-218, April 2005.
[17] A. Yumoto, T. Shinshi, X. Zhang, H. Tachikawa and A. Shimokohbe. A One-DOF Controlled Magnetic Bearing for Compact Centrifugal Blood Pumps, Motion and Vibration Control, pp. 357-366, 2009.
[18] Q. D. Nguen, S. Ueno. Analysis and Control of Nonsalient Permanent Magnet Axial Gap Self-Bearing Motor, IEEE Trans. Industry Electronics, vol. 58, Issue 7, pp. 2644-2652, 2011.
[19] Q. D. Nguen, S. Ueno, "Modeling and Control of Salient-Pole Permanent Magnet Axial-Gap Self-Bearing Motor, IEEE/ASME Transactions on Mechatronics, Vol. 16, No.3, June 2011.
[20] S. Ueno and Y. Okada. Vector Control of an Induction type Axial Gap Combined Motor-Bearing, Proceedings of IEEE/ASME International Conference on Advanced Intelligent Mechatronics, Atlanta, USA, Sep. 19-23, 1999.
[21] J. Asama, Y. Hamasaki, T. Oiwa, and A. Chiba. Proposal and Analysis of a Novel Single-drive Bearingless Motor, IEEE Transactions on Industrial Electronics (in press).